Structural and Thermal Analysis of the ORCASat

João Pedro de Prata Neves Duarte
joao.prata.duarte@tecnico.ulisboa.pt

Instituto Superior Técnico, Universidade de Lisboa, Portugal

January 2020

Abstract

Structural and thermal analysis of the Optical Reference Calibration Satellite (ORCASat), a 2U CubeSat. The goal is to demonstrate that the spacecraft fulfills the mechanical and thermal requirements during launch and orbital conditions. On the structural level, it is verified if the satellite's fundamental frequency remains above 90 Hz and if its main structure handles a load of 1200 N along the longitudinal axis. *Siemens NX Nastran* is used for both vibration and linear static analysis. Solutions are proposed when the requirements are not fulfilled. The numerical data is compared with the results obtained by two experimental tests - a shaker test performed at the University of Victoria and an impact test performed at the National Research Council. After an improvement involving the density of the material Aluminum 6061, the FEM model representing the spacecraft's external structure is validated. On the thermal level, the components' thermal cycles are studied to verify if the ORCASat operates between the safe temperature range in the defined orbit. The solver *Siemens NX Space Systems Thermal* is used in this analysis. Boundary conditions such as *Radiation Simulation Object*, *Heat Loads* and *Orbital Heating* are described and established. Simplifications in the solution details are suggested. Two opposite cases are analysed – hot and cold case – where a passive thermal control system is developed to maintain the ORCASat between its operational temperatures. It is proven that this satellite can maintain its structural integrity after launch and survive the space environment, being operational during its lifetime.

Keywords: CubeSat; Finite Element Model; Structural Analysis; Fundamental Frequency; Thermal Analysis; Thermal Control System

1. Introduction

Satellites surround us and have an active role in our quotidian with different purposes like military (e.g. espionage), scientific (e.g. meteorology) or commercial (e.g. telecommunications). To better understand the universe, more accurate instruments are needed. Orbital measurements done by satellites cover wider areas and show more precise results than the data obtained by ground-stations on Earth or even airborne observations because the atmosphere interference is lower or null.

The Optical Reference Calibration Satellite (ORCASat) is a nanosatellite being developed through a combined effort of three western Canadian universities – University of Victoria (UVic), Simon Fraser University (SFU) and University of British Columbia (UBC) - with the collaboration of the Canadian Space Agency (CSA). It is part of a contest named Canadian CubeSat Project and shall be launched from the International Space Station in the final quarter of 2021.

Nanosatellites have a mass varying from 1 to 10 kg and the dimensions are very small when compared to other groups of satellites [7]. Since they can be launched as secondary payloads, the development period is shorter and, nowadays, is possible to fit more complex instruments in less space, these nanosatellites start gaining importance as great science advances could be made at lower cost [10]. The ORCASat adopts a CubeSat configuration and is composed by 2 units, with the dimensions of $10\times10\times22.7$ cm and a maximum mass of 3.6 kg. The spacecraft shall provide a reference light source in Low Earth Orbit (LEO) to test a novel methodology for calibrating ground-based optical telescopes and shall supply the Canadian Hydrogen Intensity Mapping Experiment (CHIME) observatory by calibrating its observation antenna.

With two years prior to launch, this work was developed while the preparation for the Preliminary Design Review (PDR) presentation. The goal is to characterize the ORCASat's behaviour on the structural and thermal level. Finite element analysis were performed in order to know this behaviour and solutions were adopted every time its integrity

and components were not working at the safe range. This was possible using the CAD model developed by the *Mech* team.

In the structural analysis the FEM models are developed from the simplest to the most complex and modal simulations are performed to check the satellite's fundamental frequency and respective mode shapes. In order to validate the models used, these results are then compared with three different experimental tests. If at any time the results do not meet the requirements, a solution should be proposed. If the error between the experimental and numerical results is significant, the numerical model needs to be updated so that better and more reliable data on future numerical analysis can be obtained.

In the thermal analysis the satellite is simulated in an orbit with the same characteristics as the real one. The thermal cycles of each component are analyzed and if the temperatures are outside their safe range, solutions should be proposed as well.

The data and results obtained during this work should not be considered as final results but should help the team to evaluate if the mission is going towards success.

2. Theoretical Background

2.1. Dynamic Analysis

2.1.1 Numerical Modal Analysis

The main purpose of a numerical modal analysis is to determine the natural frequencies and respective mode shapes of a system allowing to evaluate its dynamic characteristics [5]. The fundamental frequency is the first natural frequency and the most relevant being its value influenced by a great number of factors related to the physical properties of the system, applied boundary conditions, magnitude and distribution of masses and inertia.

A multidegree-of-freedom system can have its equations of motion represented in a matrix form that depends on the mass matrix $\mathbf{M}$, the damping matrix $\mathbf{C}$, the stiffness matrix $\mathbf{K}_e$ and the force vector $\mathbf{F}$, being $\mathbf{x}$, $\dot{\mathbf{x}}$ and $\ddot{\mathbf{x}}$ the displacement, velocity and acceleration, respectively [9].

$$\mathbf{M}\ddot{\mathbf{x}} + \mathbf{C}\dot{\mathbf{x}} + \mathbf{K}_e\mathbf{x} = \mathbf{F} \tag{1}$$

To determine the natural modes of vibration the force is zero. The undamped free vibration system is represented by,

$$\mathbf{M}\ddot{\mathbf{x}} + \mathbf{K_e}\mathbf{x} = 0 \tag{2}$$

Assuming that,

$$\mathbf{x} = \phi_{\mathbf{v}} sin(\bar{\omega}t + \varphi) \tag{3}$$

which corresponds to an harmonic solution. Replacing in the Eq.2, the eigenvalue problem is obtained,

$$(\mathbf{K}_e - \bar{\omega}^2\mathbf{M})\phi_{\mathbf{v}} = 0 \tag{4}$$

A non-trivial solution for this problem is given,

$$\det(\mathbf{K}_e - \bar{\omega}^2\mathbf{M})\phi_{\mathbf{v}} = 0 \tag{5}$$

where $\bar{\omega}^2$ defines the eigenvalues and $\phi_{\mathbf{v}}$ defines the eigenvectors allowing to obtain the natural frequencies and natural mode shapes, respectively. The natural frequencies, in *Hz*, can be calculated from,

$$f_i = \frac{\bar{\omega}_i}{2\pi} \tag{6}$$

If the system presents damping, each frequency of damped vibration can be computed using,

$$\bar{\omega}_{d_i} = \bar{\omega}_i\sqrt{1-\zeta_i^2} \tag{7}$$

being ζ the modal damping ratio and obtained by,

$$\zeta_i = \frac{c_i}{2m_i\bar{\omega}_i} \tag{8}$$

where c_i and m_i represent the damping and mass terms of the correspondent equation. An oscillatory motion only results if $\zeta < 1$, which corresponds to the underdamped case. The frequency of the damped vibration is always lower than the natural frequency [4].

2.1.2 Experimental Modal Analysis (EMA)

A purpose of doing a numerical analysis using a finite element method is being able to compare the data and validate the model with the results obtained by experimental tests. Shaker and impact testing can be performed [8]. The shaker test consists of placing and attaching the structure on a shaker table that will input a force in a certain frequency range. Impact test uses an hammer to excite the system. Both tests measure the displacement, velocity or acceleration at specific points and the data is obtained as Frequency Response Functions (FRFs) which is a ratio of the structure's behavior (output) due to the applied force (input), transformed from the time domain to the frequency domain using Fast Fourier Transform (FFT) algorithms. The resonance frequencies are identified as the peaks of the amplitude diagrams.

2.2. Thermal Analysis

This analysis simulates the space environment and, by defining the orbit parameters, it is possible to know the variations of temperature that occur on the spacecraft as well as if its components stay between their operational range. An heat balance is established where all the energy exchanges are considered.

In LEO, the atmosphere rarefaction is significant so the convection can be neglected. Conduction and

radiation take an important role in the heat balance. The net heat rate is given by [6],

$$\dot{Q}_{net} = \dot{Q}_{in} - \dot{Q}_{out} + \dot{Q}_{generation} \tag{9}$$

where,

$$\dot{Q}_{net} = mc_p \frac{\delta T}{\delta t} \tag{10}$$

The rate of heat transfer that enters the system by radiation has several sources as the solar radiation, Earth's infrared radiation and albedo and radiation from the surroundings. Since the ORCASat has different components with different surfaces, each one will absorb distinct fractions of this radiation. Considering a component c and a surrounding body i,

$$\dot{Q}_{solar\ absorbed} = \alpha_{solar} F^c_{Sun} A_{sun} \dot{q}_{solar} \tag{11}$$

$$\dot{Q}_{albedo\ absorbed} = \alpha_{solar} F^c_{Earth_{sunlit}} A_{Earth} \dot{q}_{albedo} \tag{12}$$

$$\dot{Q}_{infrared\ absorbed} = \alpha_{infrared} F^c_{Earth} A_{Earth} \dot{q}_{infrared} \tag{13}$$

$$\dot{Q}_{surroundings\ absorbed} = \alpha_{infrared} \sum_i F^c_i A_i \dot{q}_i \tag{14}$$

being,

$$\dot{q}_{solar} = \sigma T_s^4 \tag{15}$$

$$\dot{q}_{albedo} = BAF^{Sun}_{Earth} \dot{q}_{solar} \tag{16}$$

$$\dot{q}_{infrared} = \alpha_{solar} F^{Sun}_{Earth} \dot{q}_{solar} \tag{17}$$

$$\dot{q}_i = \sigma \varepsilon_i T_i^4 \tag{18}$$

The general equation for the view factor calculation between two surfaces is given by,

$$F^j_i = \frac{1}{A_i} \int_{A_i} \int_{A_j} \frac{\cos\theta_i \cos\theta_j}{\pi R^2} dA_i dA_j \tag{19}$$

The rate of heat transfer that leaves the component c is,

$$\dot{Q}_{emitted} = \sigma A_c \varepsilon_c T_c^4 \tag{20}$$

Considering the conduction, the rate of heat transfer that enters or leaves the system is given by,

$$\dot{Q}_{conduction} = -\sum_i \frac{T_j - T_i}{\frac{L_i}{k_i A} + R_{contact} + \frac{L_j}{k_j A}} \tag{21}$$

Since the electrical components are not perfect electric current conductors, electrical energy is converted into thermal energy. The rate of heat generation by Joule Effect is,

$$\dot{Q}_{internal} = UI \tag{22}$$

3. Stuctural Analysis

Using *Siemens NX 9.0*, two solutions are chosen to verify if the ORCASat fulfill the main structural requirements.

Solution 103 - Real Eigenvalues is responsible for the dynamic behaviour where modal frequencies and respective mode shapes are obtained. It is possible to understand if the fundamental frequency is above 90 *Hz*.

Solution 101 Linear Statics – Global Constraints is responsible for the static behaviour. It is studied if the spacecraft can handle a load of 1200 N along the rails.

Having the CAD model provided, the several parts are idealized, the mesh is created, the materials assigned, the boundary conditions established and the contacts between components applied.

3.1. Finite Element Analysis

A bottom-up approach was adopted since the satellite consists on a large number of parts assembled together that requires a significant number of contacts and connections between them. Three FEM models were developed and their mesh consist of 1D, 2D and 3D elements (Figs. 1 and 2) - 1D elements represent the screws; 2D elements are used for shell surfaces resulted from the idealization process such as solar cells and; 3D elements are used for the rest of the ORCASat components.

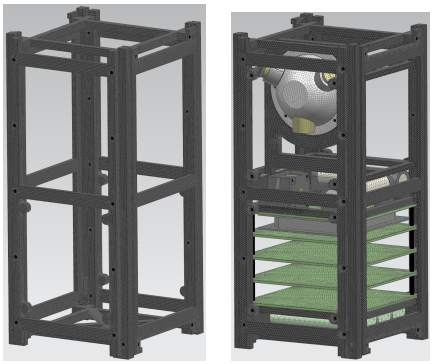

Figure 1: FEM model 1 and FEM model 2

Regarding the dynamic analysis, two different sets of boundary conditions were implemented - satellite fixed along its rails representing the case where no clearance exists between the spacecraft and the deployer and; satellite with fixed bases representing the case where this clearance exists. The fundamental frequencies obtained for the three FEM models are presented (Table 1).

The same fundamental frequency was obtained in the last model for both boundary conditions demonstrating that the rails do not have any contribution on the ORCASat's first mode of vibration. The convergence study is presented (Fig. 3) and the respective mode shape (Fig. 4).

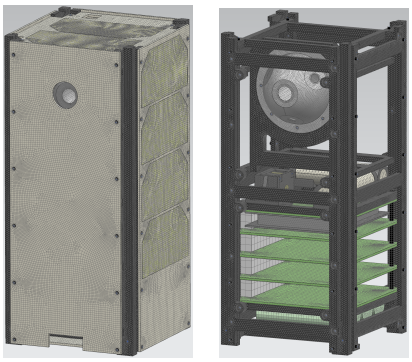

Figure 2: FEM model 3

Table 1: Fundamental Frequencies for each FEM

	Fixed Bases		Fixed Rails	
	Freq. $[Hz]$	Nº Nodes	Freq. $[Hz]$	Nº Nodes
FEM 1	728.1	557 996	1297	292 342
FEM 2	433.3	633 968	454.3	633 968
FEM 3	246.8	839 325	246.8	839 325

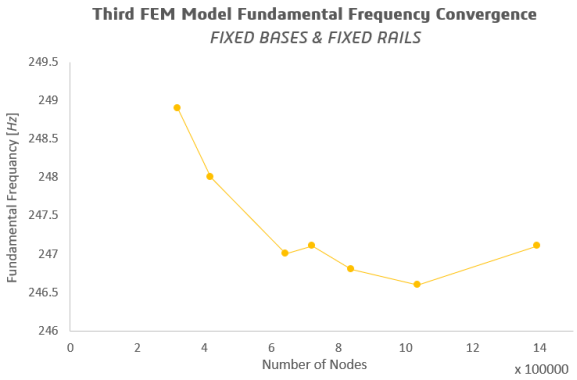

Figure 3: FEM 3 Fundamental Frequency Convergence

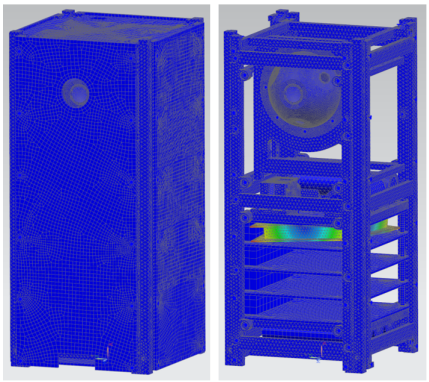

Figure 4: FEM 3 Results

To have a validation of the numerical results or to improve the accuracy of the computational models, an experimental test must be done.

Regarding the linear static analysis, the main structure was studied (Fig. 5). Applying the force on the top or bottom with fixed end showed different but approximated results (Table 2).

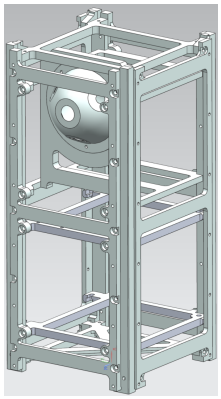

Figure 5: ORCASat's main structure

Table 2: Stress analysis

	Force on Top	Force at the Bottom
Nº Nodes	526 916	
stress-elemental $[MPa]$	11.627	11.696
stress-elemental-nodal $[MPa]$	22.71	27.52

It was concluded that the ORCASat's structure can handle the load perfectly. The values for the *stress elemental – Von Mises* are under the stress required for the aluminum to start showing plastic deformations. The yield strength of aluminum 6061 is 241.7 *MPa*.

3.2. Experimental Modal Analysis (EMA)

3.2.1 Vibration Test Performed at UVic

The system was submitted to a shaker test (Fig. 6) and is composed by the ORCASat's outer structure purely made of aluminum 6061 with stainless steel screws.

To attach the system to the shaker, a plate made of the same material was used. All adaptations were considered in the FEM model as well.

Five instruments were needed to perform the test: shaker (**2**), oscilloscope (**3**), accelerometer (**4**) (attached to the structure with wax (**1**)), function generator (**5**) and amplifier (**6**).

After attaching the accelerometer in the defined locations, which were determined considering the modal shape characteristics obtained on *Siemens NX*, the fundamental frequency revealed a value of 167.2 *Hz*. The adapted FEM model showed a value of 218.1 *Hz* (Figs. 7 and 8) which represents an error of 30.4%. Since this error is a consequence of adaptations done during the preparation of the experimental test, because of the subjectivity while

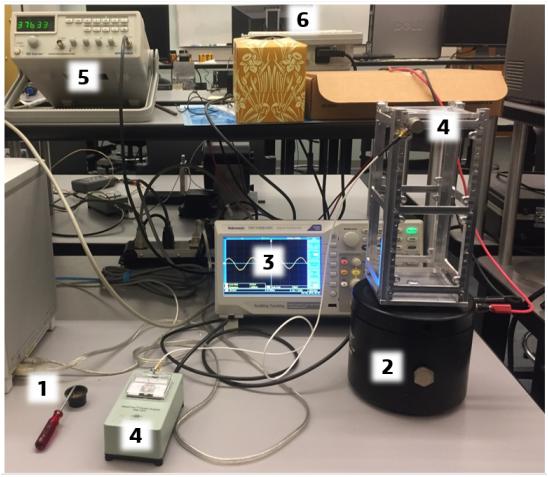

Figure 6: UVic vibration test setup

detecting the modal frequencies and because it was performed by students, another analysis was developed at the NRC installations by specialists.

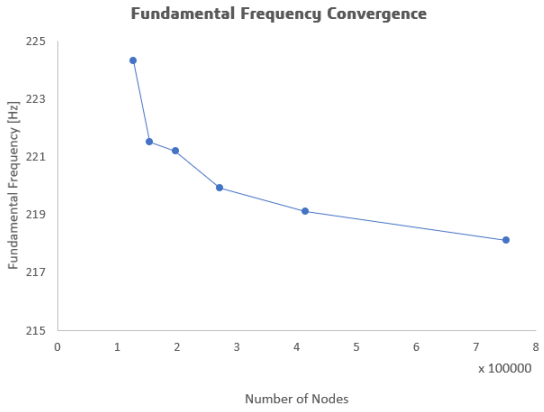

Figure 7: Fundamental frequency convergence

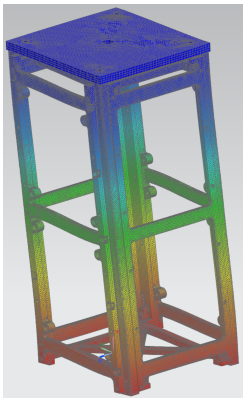

Figure 8: UVic test FEM result

3.2.2 Vibration Test Performed at NRC

This experimental vibration test was performed at the National Research Council, in Ottawa. The system was submitted to an impact test and is composed by the ORCASat's outer structure purely made of aluminum 6061 with stainless steel screws.

This free-free vibration test required the use of an excitation hammer with embedded load cell (Fig. 9). The structure was suspended using four thin wires attached to the four corners of its frames (**1**) and a bungee cord (**2**) which was connected to a firm supporting structure. 12 tri-axial accelerometers were attached to the top, mid and bottom of the structure (**3**) and the energy was analysed and confirmed to cover the target frequency range up to above 2 *kHz*. Two datasets were measured, one with the hammer at the top corner and the other with the hammer at the bottom corner (Fig. 10).

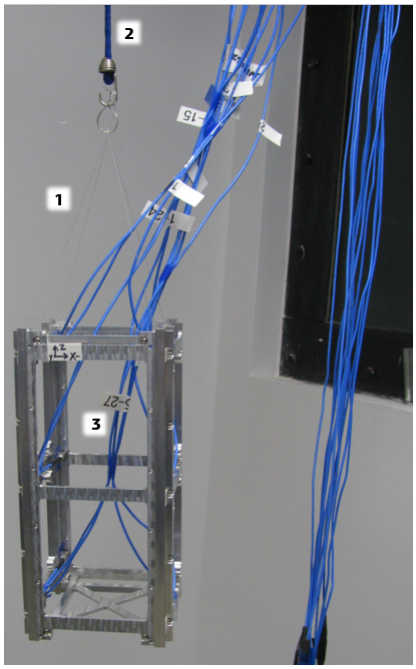

Figure 9: NRC vibration test setup

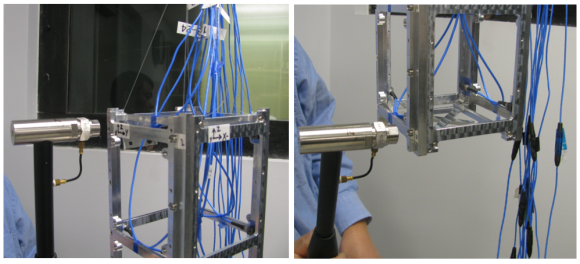

Figure 10: Impact hammer locations

The FEM model was adapted to these conditions as well. The mass of the accelerometers was

considered but dissipated to the whole model and not localized in the same area where they were placed during the experiment. The density of the aluminum 6061 was changed from 2711 kg/m^3 to 2859.81 kg/m^3 to approximate the real and numerical models.

While performing the test, all target modes were identified clearly with consistency and correlated well. NRC detected the first 9 modes of vibration. The error between the modal frequencies obtained on *Siemens NX* and NRC are presented (Table 3).

Table 3: Error between the numerical and real data

Mode	NX [Hz]	NRC [Hz]	Error [%]
1	470.8	459	2.57
2	567.5	527	7.68
3	722.1	672	7.46
4	813.2	799	1.78
5	905.4	861	5.16
6	1025	990	3.54
7	1201	1155	3.98
8	1225	1222	0.24
9	1273	1347	5.49

Despite all the approximations and induced errors that could appear during the real and simulated tests, the error is always below 8%. In fact, for the fundamental frequency, the error is, approximately, 2.6% which validates the numerical model for future analysis.

3.2.3 Vibration Test Performed at NRC (Homathko)

This test is mentioned simply for comparison and discussion between the results regarding the third FEM model and the experimental ones obtained for the satellite Homathko at NRC on July, 2018. It is relevant since is the only experimental test covering a complete model.

Homathko is a 3U CubeSat, born in the Canadian Satellite Design Challenge (CSDC) competition with a payload similar to ORCASat. The system was submitted to a free vibration test being divided in three phases - a sine sweep test from 5 Hz to 2200 Hz to identify the resonance frequency; a random vibration test to simulate the launch conditions and; another sine sweep to verify any resonance frequency changes.

The fundamental frequency was detected with a value of 130.1 Hz. Comparing with the fundamental frequency obtained for the third FEM model (246.8 Hz), it was expected that the ORCASat's frequency would be higher than the Homathko's since the latter is heavier. Homathko (3U) satisfies the requirement regarding the minimum frequency. It is reasonable to predict that a complete ORCASat (2U) will also satisfy it since both were built with the same requirements and similar features on the structural level.

3.3. Preliminary Design Review FEM Model

The model presented during the PDR presentation had some different features from the CAD model used during the numerical vibration analysis such as the inclusion of solar sensors, antenna deployer mechanism and more components in the payload module.

A vibration analysis was performed for the PDR model as well with the purpose of verifying if the ORCASat's fundamental frequency remained above 90 Hz. No component was removed from the model (Fig. 11). The system had its bases fixed and the fundamental frequency revealed that the ORCASat did not fill the requirement. This was unexpected since the third FEM model revealed a fundamental frequency above 200 Hz.

As the biggest difference between both models relies on the payload module, by analysing the mode shapes, it was concluded that the vertical payload PCB should be attached to the respective 1U brackets.

After applying this constraint, new results were obtained revealing this solution as a success (Table 4). As the structure became more stiffed, the first frequency was no longer characterized by a deformation on the vertical payload PCB (Fig. 12).

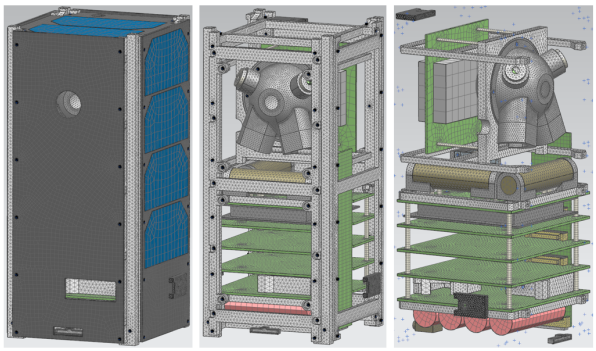

Figure 11: PDR FEM model

Table 4: Modal frequencies of the PDR model before and after applying the proposed solution

	Before	After
Number of Nodes	660	179
Mode 1 [Hz]	89.66	192.2
Mode 2 [Hz]	140.6	276.7
Mode 3 [Hz]	192.3	289.5

4. Thermal Analysis

The thermal analysis was performed using the program *Siemens NX* with the solver *Space Systems*

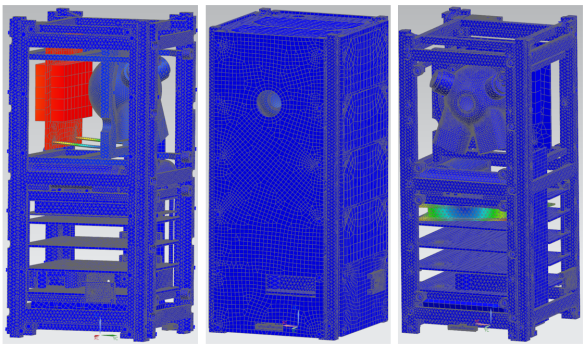

Figure 12: Mode shapes of the PDR model before and after applying the proposed solution

Thermal. In this study, only one model was used, identical to the third FEM model in the structural analysis. The idealization process is considered, the mesh is created, the materials assigned, the contacts between components applied and the boundary conditions established where the orbit, thermal loads between components and radiation are defined. Two opposite cases were analyzed - hot case and cold case - being a thermal control system developed to maintain all components within their safe temperature range.

4.1. Finite Element Model

The mesh of the thermal model is constituted by 2D and 3D elements. 2D elements were used to model the solar cells which were represented as shell surfaces. 3D elements were used in the rest of the satellite's components. 1D elements were not used in this FEM model since all contacts were considered as perfect and the surfaces glued.

Regarding the printed circuit boards, instead of applying the heat loads in the specific electronic components, these were applied to the whole PCB area since they were not modelled yet. The values for the heat loads are presented (Tables 5 and 6).

Table 5: Power specifications for Hot Case $[mW]$ and solar flux $[W/m^2]$

Hot Case	
Solar Flux	1411.426
ADCS PCB	750
ADCS Magnetorquers (each)	3.3
TT&C PCB	25
OBC PCB	145
Payload PCB	10
EPS PCB	920
EPS Battery (each)	35
X Solar Panel (each)	135
Y Solar Panel (each)	135
Z Solar Panel	170

The satellite starts orbiting at a temperature of 15°C for the hot case and 8°C for the cold case [11].

Table 6: Power specifications for Cold Case $[mW]$ and solar flux $[W/m^2]$

Cold Case	
Solar Flux	1323.682
ADCS PCB	750
ADCS Magnetorquers (each)	3.3
OBC PCB	145
EPS PCB	410
EPS Battery (each)	25

For the *radiative environment temperature*, according to [12], $4K$ was defined.

The *maximum number of orbits* is predefined as 12 but this value was changed to 5 since it was observed that, after the first orbit, the difference in range of temperatures was minimal.

Initally, the number of samples per orbit was defined as 10 however, the plot for the temperatures evolution was not well defined. This value was altered to 15 which increased the time needed for the simulations but provided better data.

It was assumed that the external components were the only exchanging radiation with the space environment. The internal components radiate to each other. For this, *Radiation Simulation Object* was the boundary condition applied.

In the hot case, the date was defined as 21st December 2021 (at 04:00:00) and in the cold case was 22rd June 2022 (at 10:00:00). These dates were computed by establishing the exact solstice dates for 2021 and 2022 and detecting the moment with the maximum and minimum beta angle for the hot and cold case, respectively.

The orbit parameters can be visualized in the table below.

Table 7: Orbit parameters

	Cold Case	Hot Case
Orbit Period $[s]$	5549.087	
Minimum Altitude $[km]$	400	
Eccentricity (e)	0.0005	
Orbit Inclination (i) $[deg]$	51.64	
Argument of Periapsis $[deg]$	34.8042	
Local Time at Ascending Node (Ω)	10:00:00	04:00:00

4.2. Results and Conclusions

Initially, no thermal control system was applied. The solar panels had the same thermo-optical properties as the PCBs being considered as simple fiberglass epoxy materials. After obtaining the results, the only components considered as critical were the integrating sphere, momentum wheel and batteries.

The maximum and minimum temperatures obtained for both hot and cold cases are presented (Tables 9 and 10) as well as the operating temperatures of these critical components (Table 8).

A thermal control system must be implemented.

Table 8: Operational temperatures on the thermal model

Operational Temperatures [^oC]	
integrating sphere	-25 to +60
momentum wheel (bracket)	-25 to +60
batteries [3]	0 to +45

Table 9: Thermal results without TCS - Cold Case

	Cold Case	
	Min. [^oC]	Max. [^oC]
integrating sphere	-27.688	2.196
momentum wheel (bracket)	-28.441	2.964
batteries	-28.488	2.961

Table 10: Thermal results without TCS - Hot Case

	Hot Case	
	Min. [^oC]	Max. [^oC]
integrating sphere	-12.366	11.354
momentum wheel (bracket)	-13.417	12.219
batteries	-13.441	12.226

4.3. Thermal Control System

The ORCASat has power limitations and passive thermal control systems are more reliable, lighter, cheaper, easy to integrate and don't require any kind of power from the satellite so, these were the first being implemented. If the solutions adopted are not enough to maintain the critical components between their operational range and no other option exists, an active thermal control system shall be implemented.

The solar panels were considered as black surfaces instead of the usual fiberglass epoxy material and the anodized aluminum was treated with a black paint as well. These passive thermal control systems are characterized for changing the values of emissivity and absorptivity. Thus, a bigger portion of radiation is absorbed by the satellite, increasing the overall temperature of the components.

4.3.1 TCS - Black anodized aluminum and black solar panels

By applying both passive TCS, higher minimum temperatures through the cold case were obtained (Tables 11 and 12). The batteries continued outside the desired temperatures but applying an active thermal control system is a decision that should be avoided at all costs.

After discussing with both *Management*, *Mech* and *Payload* teams and studying other possible solutions, a new type of batteries with the capability of recharging under -35°C was considered.

Table 11: Thermal results with TCS - Cold Case

	Cold Case	
	Min. [°C]	Max. [°C]
integrating sphere	-20.325	18.033
momentum wheel (bracket)	-21.216	19.120
batteries	-21.274	19.120

Table 12: Thermal results with TCS - Hot Case

	Hot Case	
	Min. [^oC]	Max. [^oC]
integrating sphere	-1.211	30.855
momentum wheel (bracket)	-2.625	31.990
batteries	-2.644	31.997

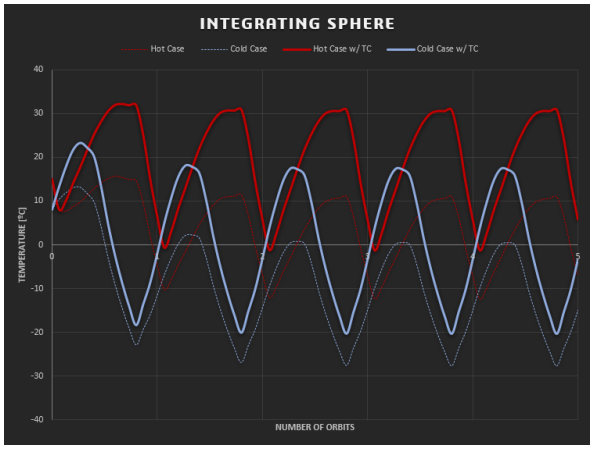

Figure 13: Integrating sphere thermal cycle

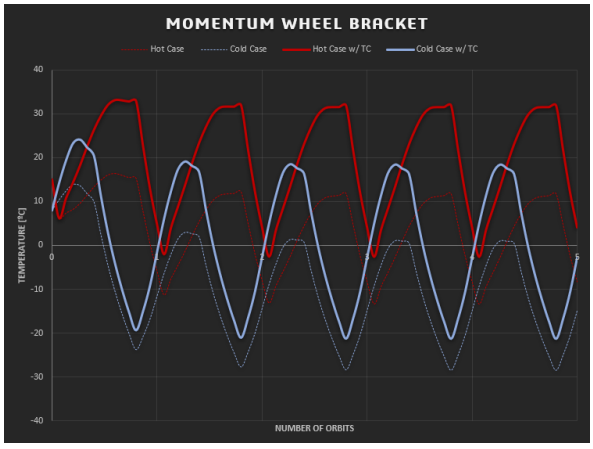

Figure 14: Momentum wheel thermal cycle

4.4. New batteries

The initial batteries were lithium-ion from *Panasonic* charging between 0 and +45°C. The new batteries are lithium-titanate being able to recharge at -40°C. They present a longer life cycle compared to lithium-ion of 3000 to 7000 charge cycles and higher security, stability and charge faster. However, they present lower inherent voltage of 2.4V/cell leading to a lower energy density [1]. The values for the recharge efficiency and capacity are presented (Table 14) as well as the conditions of the experimental test performed by Hunan Huahui New Energy Co. (Table 13).

Table 13: Experimental test conditions on lithium-titanate battery cells [2]

Test Conditions	
Items	Descriptions
Sample models	LTO cell 18650 1.3Ah 2.4V
Room temperature $[^oC]$	25 ± 2
Humidity $[\%]$	35-75
Test methods	After the cells are discharged, charge with constant current and constant voltage at 25°C / -20°C / -30°C / -35°C / -40°C

Table 14: Experimental test results on lithium-titanate battery cells [2]

Record capacity datas		
Test temp. $[^oC]$	Recharge efficiency $[\%]$	Capacity $[\%]$
25	100	100
-20	97	88.5
-30	83.6	66.7
-35	62.6	35.7
-40	49.5	15.1

This is a viable solution that must be implemented to the ORCASat, solving the problem related to low battery temperatures. It is observed that the efficiencies are low when LTO batteries recharge at -40°C. Nevertheless, the peaks of temperature with both passive TCS applied show that the worst cold case happens above -25°C with an efficiency of, approximately, 97% and a capacity, compare with 25°C, of 88.5%.

This type of batteries is being analyzed and evaluated by NanoRacks to verify if their composition presents any hazard to the space environment. After the Preliminary Design Review presentation, NanoRacks did not provided any information or conclusions on this matter, being the batteries still under study.

5. Conclusions

In the structural analysis, the three models showed that the ORCASat is able to maintain its physical integrity during launch being the fundamental frequency above $90Hz$ on both boundary conditions applied. With the static study performed on the satellite's main structure, it was theoretically verified that the ORCASat can withstand a force of 1200 N along its length.

This analysis was performed on the model presented in the Preliminary Design Review presentation as well. Initially it was observed that the fundamental frequency had dropped below $90Hz$ however, after analyzing its modal frequencies, respective mode shapes and changing the constraints the fundamental frequency increased above this value, fulfilling the requirement.

This study is supported by three vibration experimental tests. The experimental tests done while the development of this work were performed on the outer ORCASat structure represented by the first FEM model. These tests have the same purpose, determining the fundamental frequency of the structure, but the method used was different. The first FEM model was adapted to the constraints of both tests and the validation of this numerical model was successfully obtained for the test performed at NRC. The UVic test allowed the team to be in touch with experimental instruments and to develop the knowledge regarding experimental vibration tests but, unfortunately, the error between the real and numerical models was too large. Finally, the second experimental test performed at NRC was not done while the development of this work but is presented as a way of comparison with the third FEM model. No validation can be extracted from this test but it can be demonstrated that the ORCASat is likely to have a frequency above $90Hz$.

In the thermal analysis, the third FEM model is placed in orbit, the satellite temperatures were obtained at two opposite cases, the cold case and hot case. Passive thermal control systems were applied and the spacecraft components temperatures were dragged into the operating range with the exception of the batteries. By avoiding the development of an active thermal control system due to power restrictions, the solution was to replace lithium-ion batteries by lithium-titanate. These batteries are still being analyzed by NanoRacks and the Canadian Space Agency.

All the objectives initially proposed were accomplished.

Acknowledgements

I want to thank my supervisor, Professor Afzal Suleman for giving me the opportunity to develop this project at the Centre for Aerospace Research at the University of Victoria and for the financial support.

I also want to thank Prof. Keivan Ahmadi, Prof.

Rasoul Sohouli and Prof. Vahid Ahsani from the University of Victoria; Ph. D. Viresh Wickramasinghe and Eng. Eric Chen from the National Research Council; and Frederico Alves from Instituto Superior Técnico for the orientation provided during the development of this work, for answering my questions, for helping me solving the problems and for the knowledge you transmitted.

For the people in Canada, I want to thank everyone from the ORCASat team, specially the ones that worked by my side during my stay in Victoria B.C. - Alex Doknjas, Peter Ogilvie and Tristan Tarnowski.

Last but not least I want to thank my family and friends. I do not have words to describe how grateful I am to have you in my life. A big thank you.

References

[1] AA Portable Power Corp, Category: LTO Batteries. URL https://www.batteryspace.com/Lithium-Titanate-Battery.aspx.

[2] LTO18650 1.3Ah 2.4V - Capacity Vs Temperature test. Document provided by the ORCASat manager Alex Doknjas.

[3] Panasonic Lithium Ion NCR18650B. URL https://www.batteryspace.com/prodspecs/NCR18650B.pdf, Accessed 05/06/2019.

[4] S. C. Aboobakar. Dynamic and thermal models for ecosat-iii, November 2016. Master's Thesis, Instituto Superior Técnico, University of Lisbon.

[5] J. Archer. Natural Vibration Modal Analysis. September 1968.

[6] T. L. Bergman, F. P. Incropera, D. P. DeWitt, and A. S. Lavine. *Fundamentals of Heat and Mass Transfer, Seventh Edition*. John Wiley & Sons, 2011. ISBN:978-0470501979.

[7] B. Lal and T. Zurbuchen. *Achieving Science with CubeSats: Thinking Inside the Box*. National Academy of Sciences, 2016.

[8] N. Larbi and J. Lardies. *Experimental Modal Analysis of a Structure Excited by a Random Force*, volume 14, pages 181–192. Mechanical Systems and Signal Processing, 2000.

[9] S. S. Rao. *Mechanical Vibrations, Fifth Edition*. Prentice Hall Upper Saddle River, 2011. ISBN:978-0132128193.

[10] D. Selva and D. Krejci. A survey and assessment of the capabilities of Cubesats for Earth observation. 2011.

[11] L. R. Simões. Study of low earth orbit impact on orca2sat subsystems, January 2019. Master's Thesis, University of Beira Interior.

[12] A. Tewari. *Atmospheric and Space Flight Dynamics*. Springer, 2007.